

Figure 1: Bathymetric map of the Alboran Sea showing the structural features of the area. Shaded bathymetry from compilation of ISTEP and CSIC multibeam cruises with GEBCO 2014 database, topography from SRTM database. Focal mechanism in black: 1994 main shock (El Alami et al., 1998; Biggs et al., 2006). Focal mechanism in red: 2004 main shock (van der Woerd et al., 2014). Focal mechanism in green: 2016 main shock (Kariche et al., 2017; Medina and Cherkaoui, 2017). Focal mechanism in orange: Location and moment tensor solution obtained for the 1910 Adra Earthquake from Stich et al. (2003). AF, Averroes Fault; AIFZ, Al Idrissi Fault Zone; A.Is, Alboran Island; AR, Alboran Ridge (Alboran ridge thrust front, ARTF); CSF, Carboneras Serrata Fault; EAB, East Alboran Basin; FP, Francesc Pagès Seamount; IB, Ibn-Batouta Bank; JF, Jebha Fault; NB, Nekor Basin; NF, Nekor Fault; PB, Pytheas Bank; SAB, South Alboran Basin; SAR, South Alboran Ridge; TB, Tofiño Bank; WAB, West Alboran Basin; XB, Xauen Bank; YF, Yusuf Fault. Orange dashed areas AR and SAR correspond to the two key sites of this study (Alboran Ridge and South Alboran Ridge respectively). Offshore structural features from Estrada et al. (2017); d’Acremont et al. (2020). Inset: water currents between Mediterranean Sea and Atlantic Ocean and main features of the basement. The arrows representing water masses are from Ercilla et al. (2019); AW, Atlantic Water; LMW, Light Mediterranean intermediate Water; DMW, Dense Mediterranean Water.

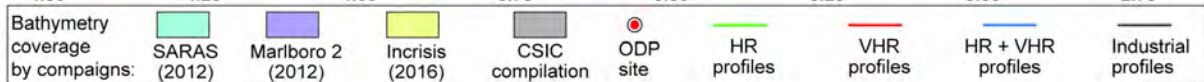
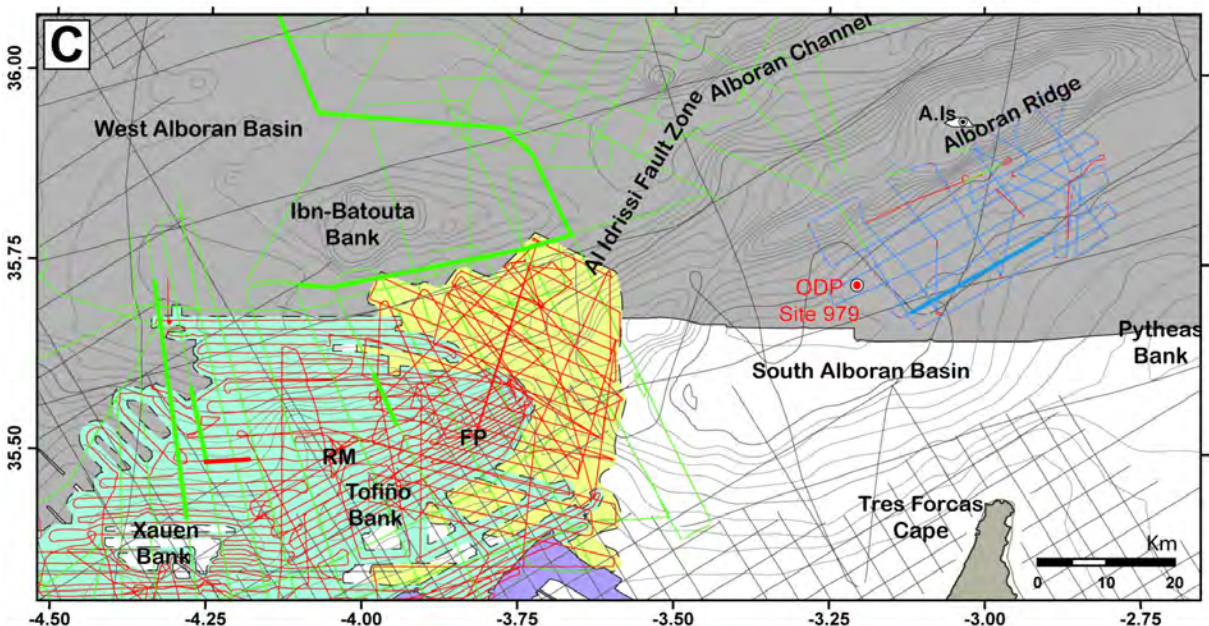
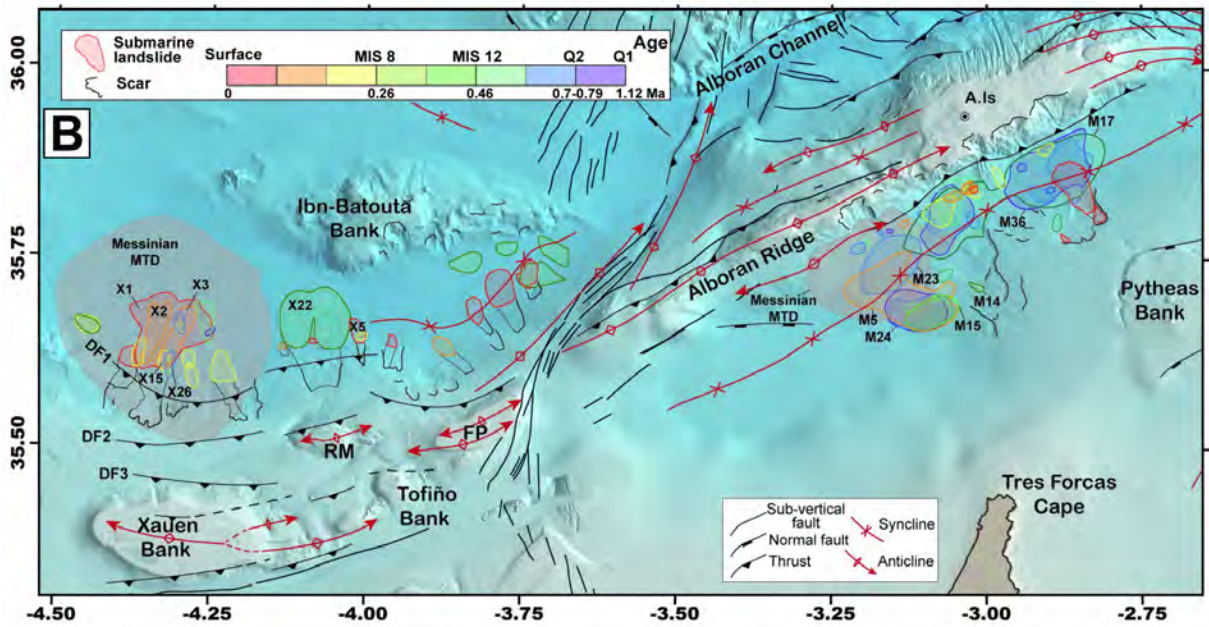
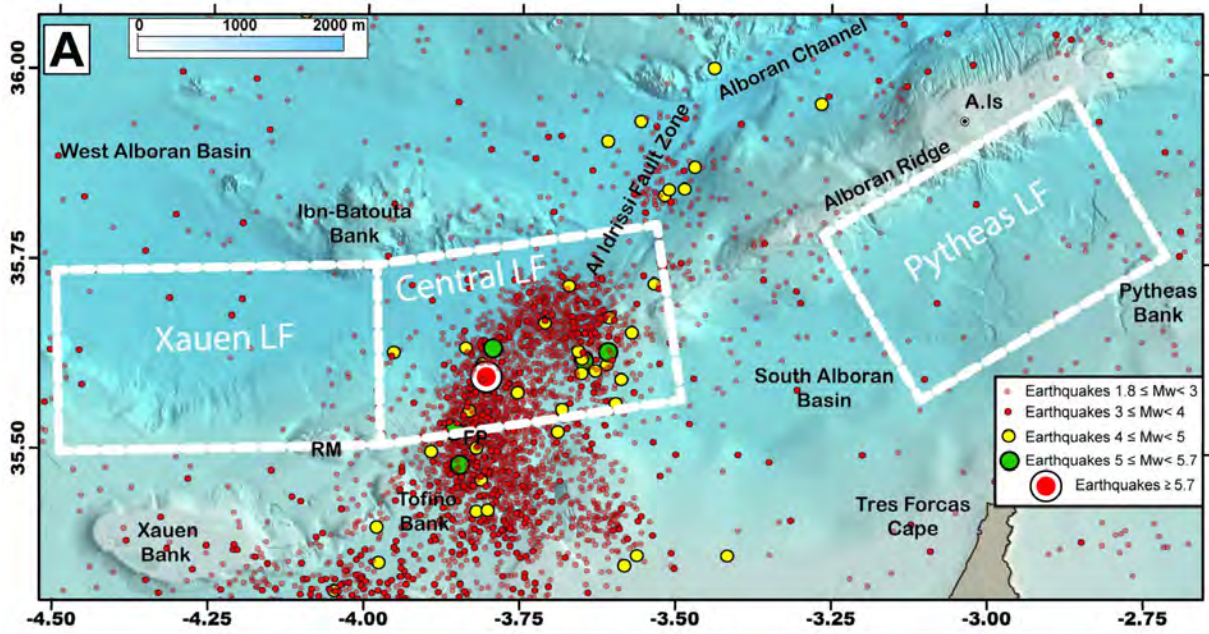


Figure 2: (A) Bathymetric and seismic epicentral map. Epicentres of the earthquakes recorded between 1964 and 2020 (Spanish Instituto Geografico Nacional (IGN) database). Landslide field location (Xauen, Central and Pytheas) is represented by the white line. Used in Figure 9. (B) Structural map (from d’Acremont et al. 2020; Lafosse et al. 2020) with the distribution of the submarine landslides from this study. Xx and Mx correspond to the code names of the MTDs described in this paper (see Appendix). DF1, DF2, DF3, deformation front highlighted by blind thrusts. A.Is, Alboran Island; FP, Francesc Pagès Seamount; RM, Ramon Margalef High. (C) Swath bathymetric and seismic reflection coverage of the study area, from CONTOURIBER (2010), Marlboro-1 (2011), Marlboro-2 (2012), SARAS (2012), MONTERA (2012), and INCRISIS (2016) projects and the Fishing General Secretary (Spanish Government) (HR: high resolution; VHR: very high resolution). Thick lines correspond to seismic reflection profiles shown in this paper.

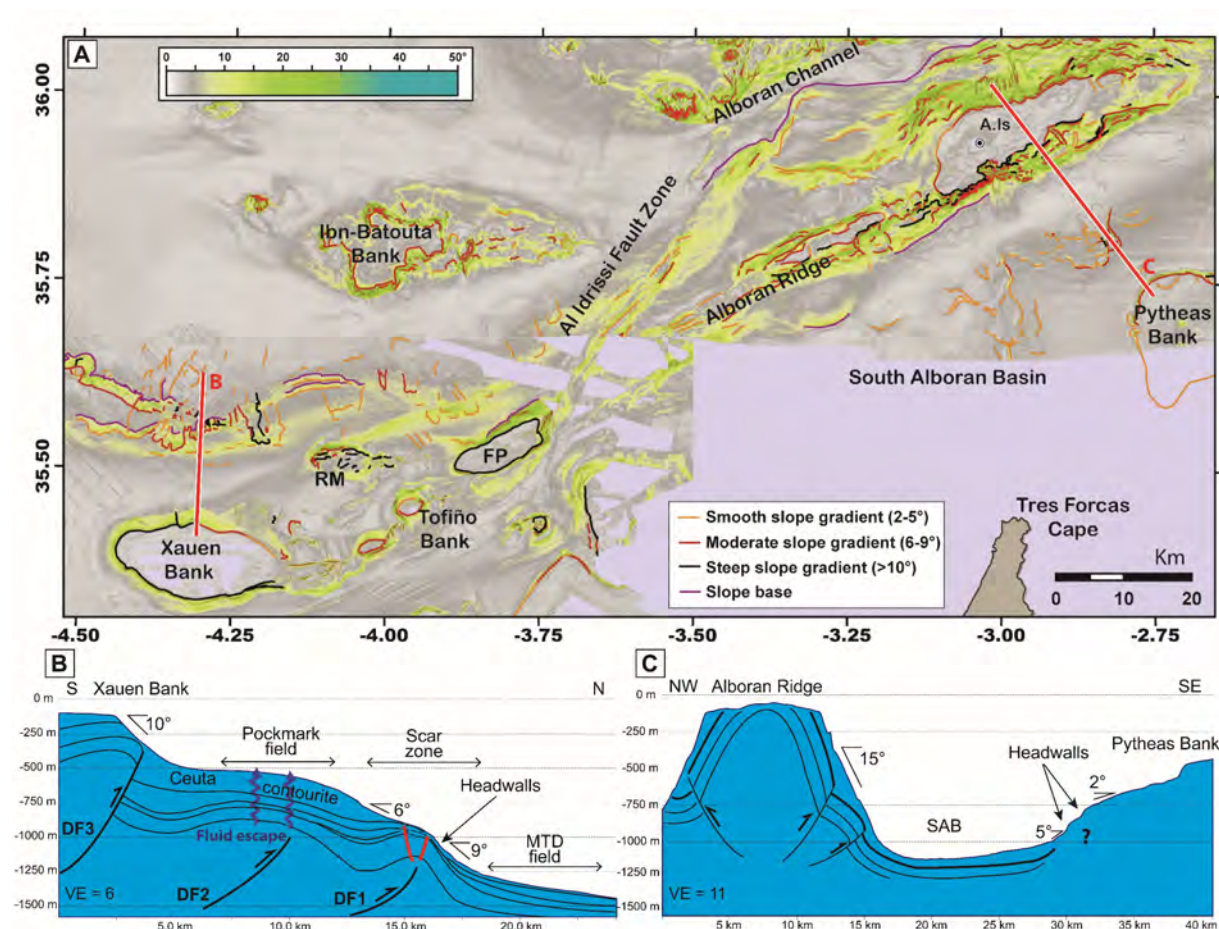


Figure 3: (A) Slope map of Southern Alboran Sea and slope failures. A.Is, Alboran Island; FP, Francesc Pagès Seamount; RM, Ramon Margalef High. (B)(C) Bathymetric profiles with structural shape, slope values are indicated (from d’Acremont et al. 2020) located north of Xauen Bank (SAR region) and transverse to the SAB from the Alboran Ridge to the Pytheas Bank (Location in A). VE, vertical exaggeration. DF1, DF2, DF3, deformation front highlighted by blind thrusts.

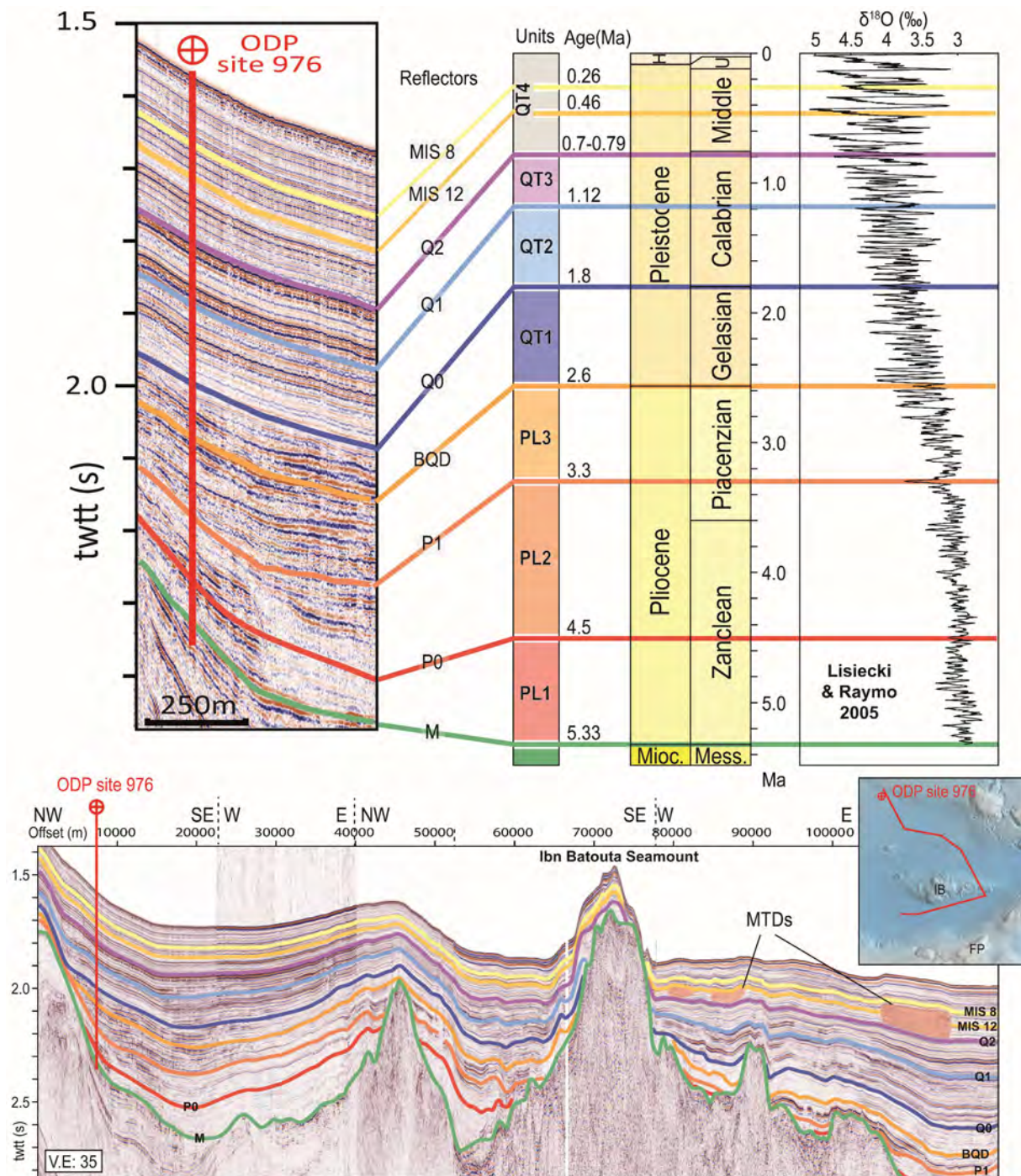


Figure 4: Chronostratigraphic units and seismic horizons using ODP sites 976 (Units from Juan et al., 2016). Benthic $\delta^{18}\text{O}$ curve from Lisiecki and Raymo (2005). Composite seismic reflection profile used to follow the chronostratigraphic units from the ODP site 976 to the study area. IB, Ibn Batouta; FP, Francesc Pagès; Mioc., Miocene; Mess., Messinian; H, Holocene; U upper. MIS 12 and MIS 8 represent Marine Isotope stages, we have used this term as the name of the reflectors.

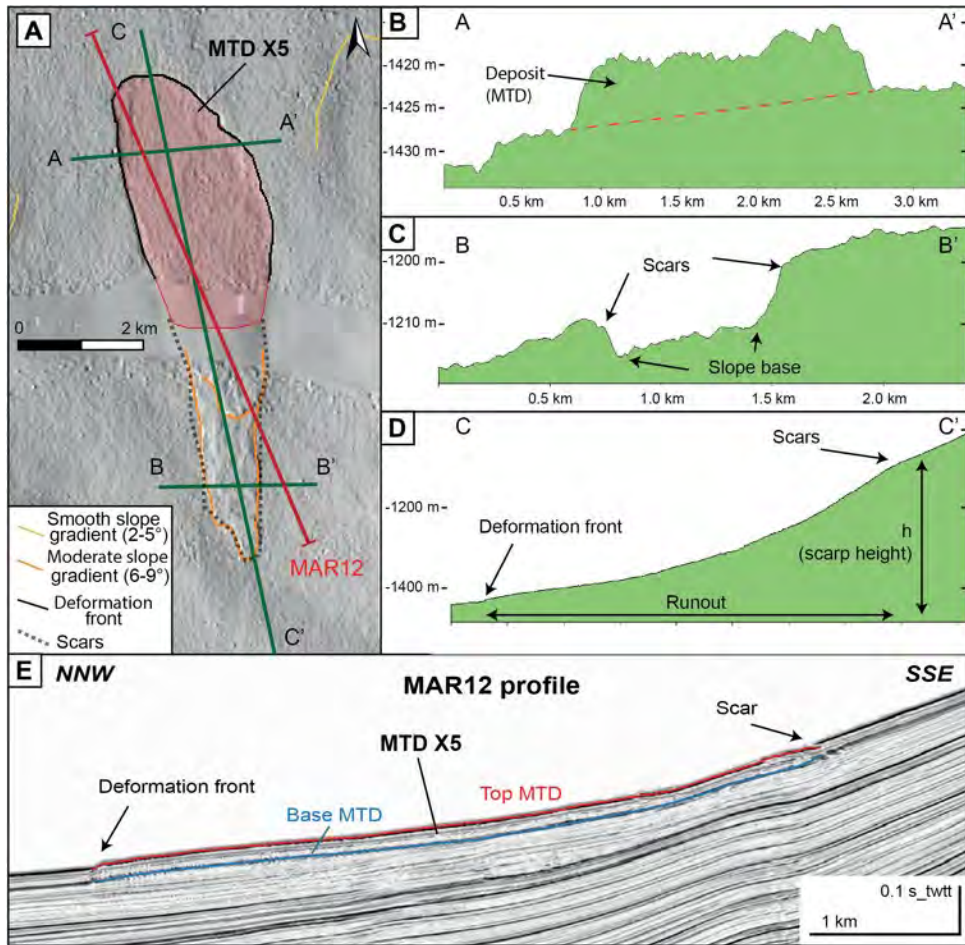


Figure 5 : Characterization of a submarine landslide using bathymetry (A), slope profiles (B, C, D) and seismic reflection profile (E): example of MTD X5 along the Xauen Bank northern flank.

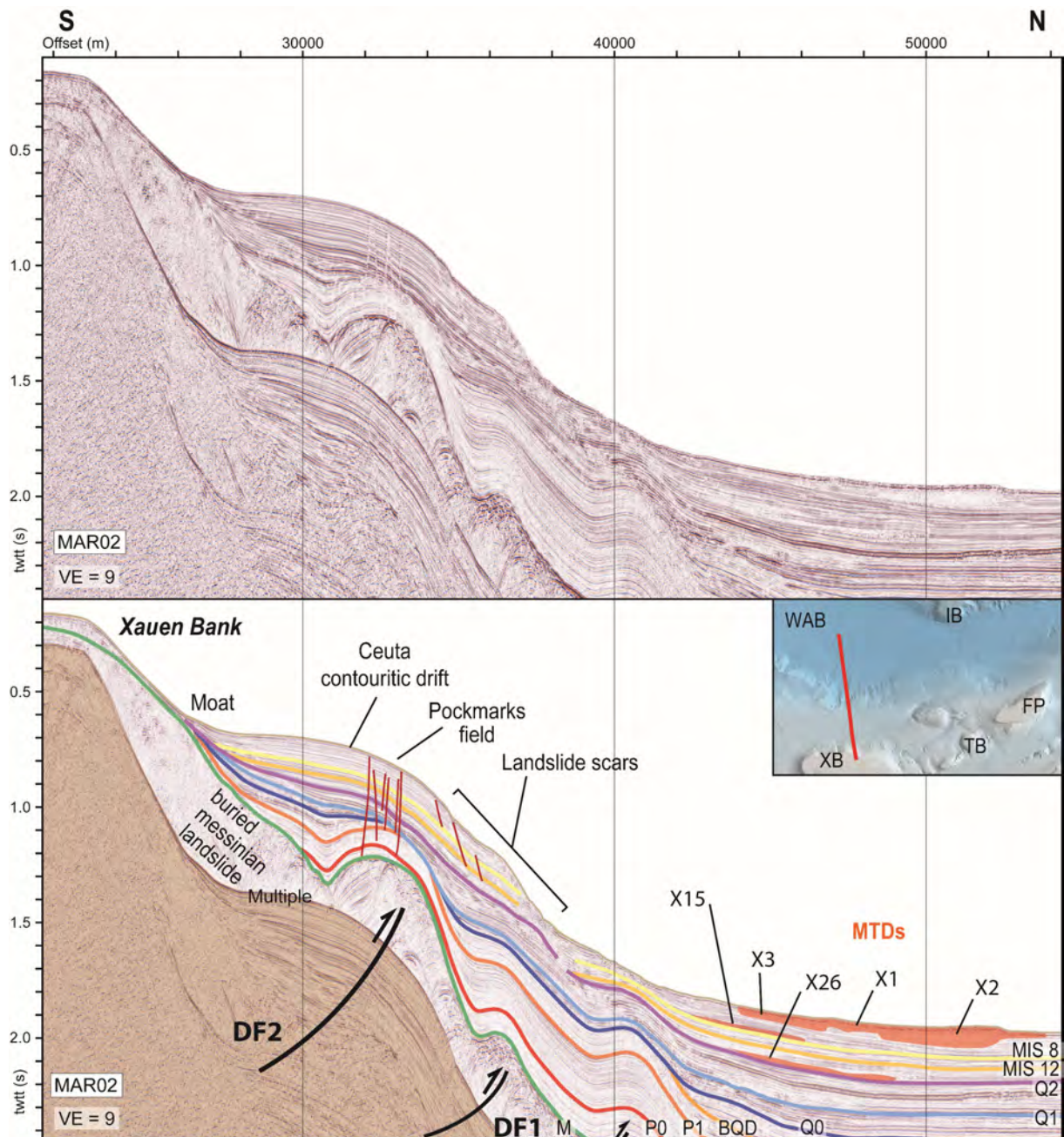


Figure 6 : High-resolution profile from Marlboro 1 campaign (MAR02), between the Xauen Bank (XB) and the southern WAB. It shows localization of landslide scars along slopes north to the Xauen Bank, where slope gradient is affected by contouritic sedimentation (Ceuta contourite drift) and northward vergence thrusts (DF1, DF2) as well as mass transport deposits (Xx mapped in Figure 2B). TB Tofiño Bank, FP Francisc Pagès Seamount, IB Ibn Batouta seamount. P0, P1, BQD, Q0, Q1, Q2, MIS12 and MIS8 refer to seismic reflectors defined in figure 4.

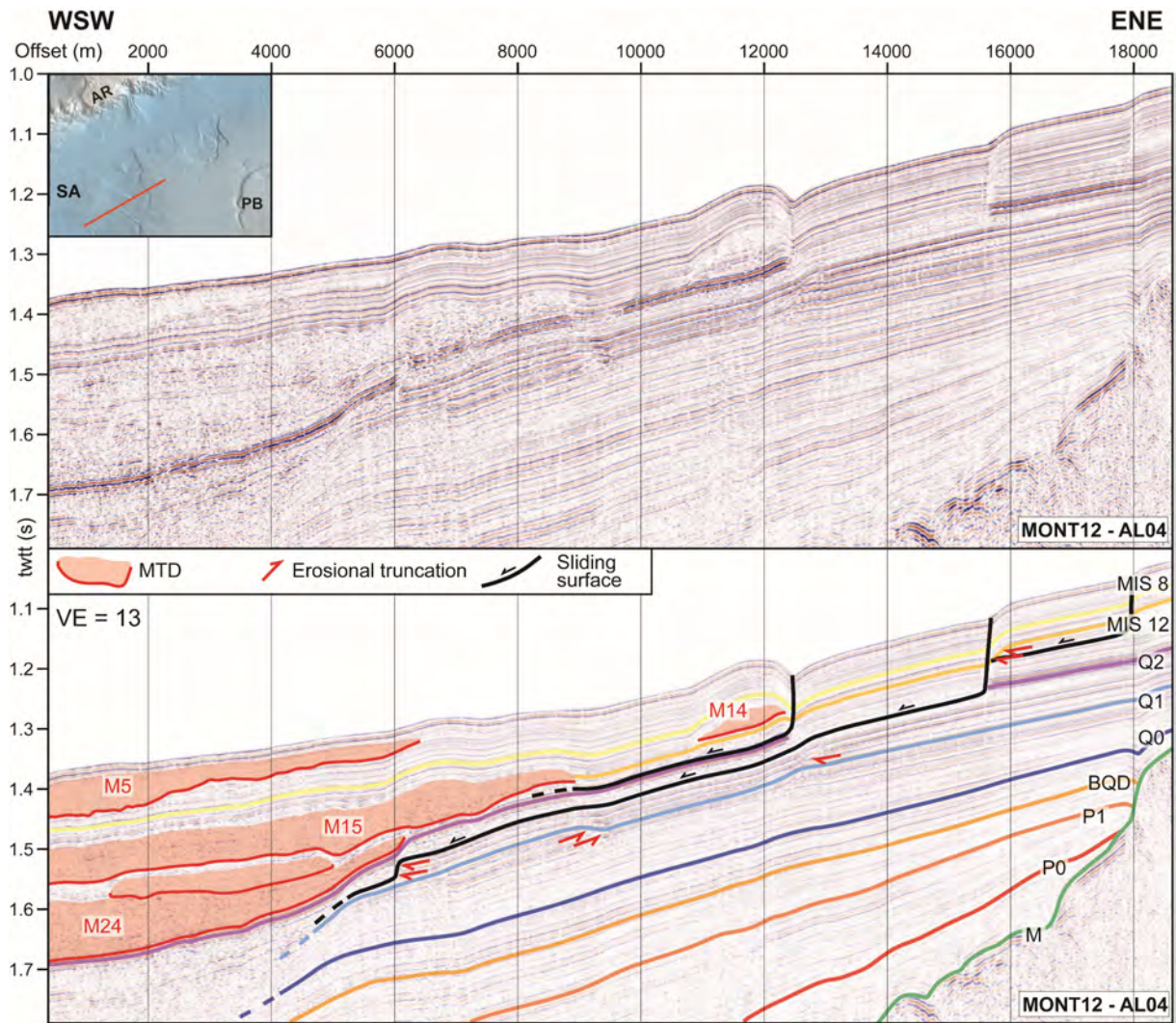


Figure 7: High-resolution profile from MONTERA campaign (AL04), in the southern SAB. It highlights buried MTDs downward the slope and three decollement levels above the Q1 reflector. Mx Mass transport deposits represented in map Figure 2B. AR Alboran Ridge, PB Pytheas Bank, M, P0, P1, BQD, Q0, xx refer to seismic reflectors defined in figure 4.

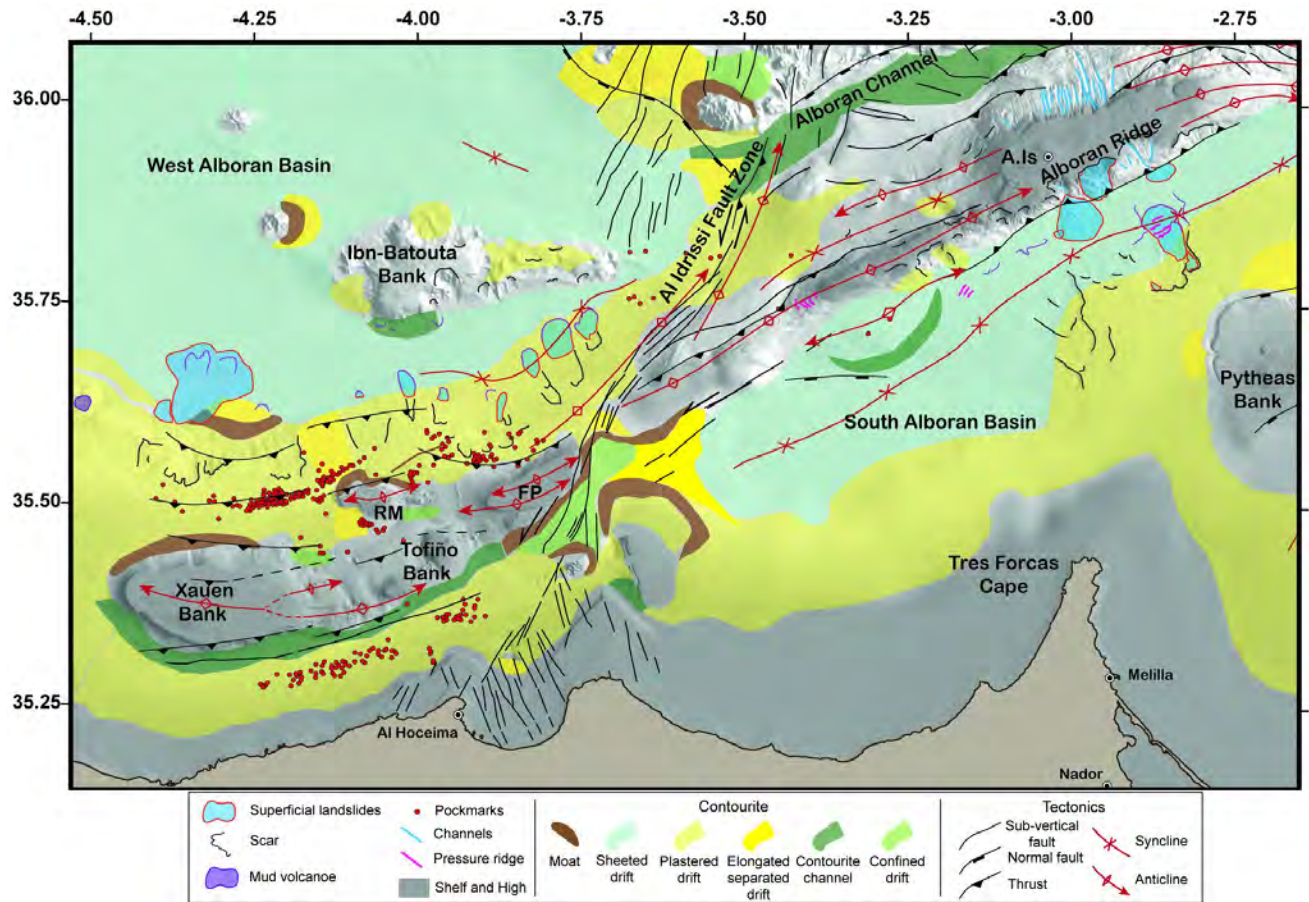


Figure 8: Morpho-structural map of the study area. Contourite deposits from *Ercilla et al. 2019*, structural features from *d’Acremont et al. (2020)* and *Lafosse et al. (2020)*. A.Is, Alboran Island; BBFZ, Boussekkour-Bokkoya Fault Zone; FP, Francesc Pagès Seamount; RM, Ramon Margalef High. DF1, DF2, DF3, deformation front highlighted by blind thrusts.

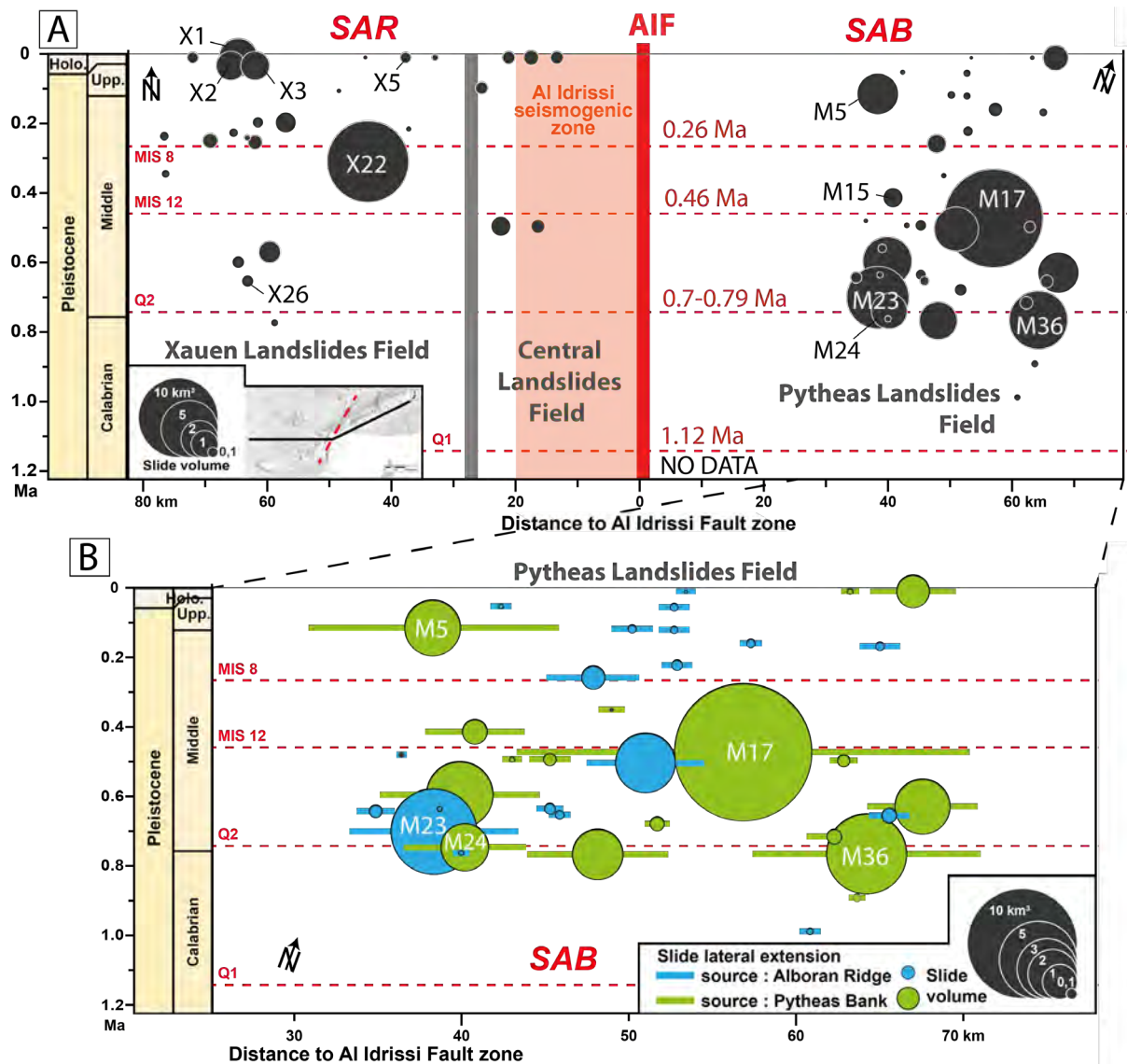


Figure 9: Distribution of landslides observed and quantified in the southern part of the Alboran Sea, west and east of the AIFZ. In the SAR region: north to the Xauen and Tofiño Banks (Xauen landslides field) and north of the Francesc Pagès Seamount (Central landslides field). In the SAB region: between the Alboran Ridge and the Pytheas bank (Pytheas landslides field). Zoom on the eastern distribution. The MTDs are represented according to their time frame, volumes and for those in the east, their sources. See Appendix A1 and A2 for MTD characteristics. Xx and Mx correspond to the code names of the MTDs described and shown in Figure 2B.

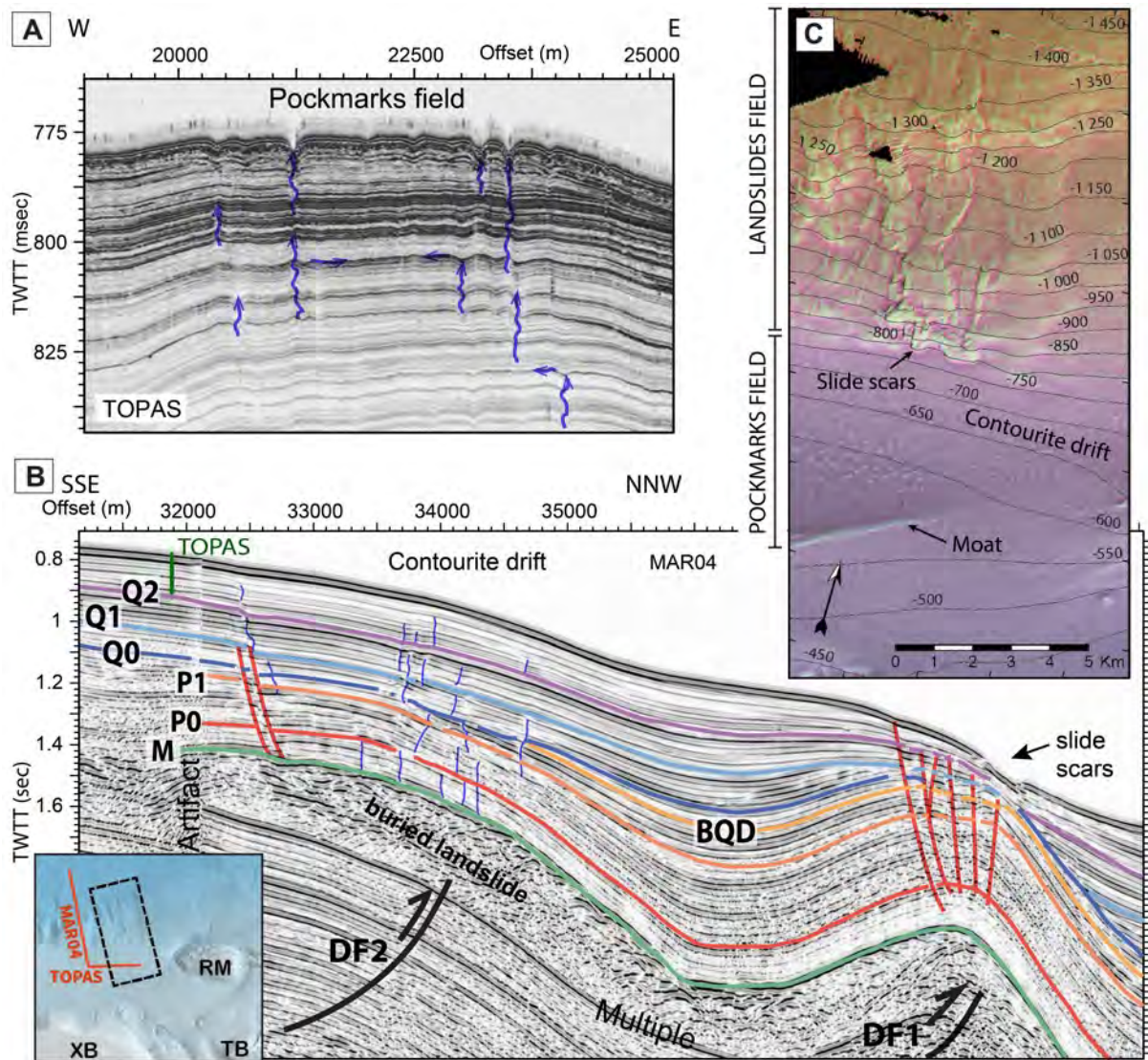


Figure 10: Fluid escape and compactional fault features through contourite drift in the SAR region (north Xauen Bank). A. Sub-seabed expression of fluid escapes and pockmarks on ultra-high resolution seismic reflection data (TOPAS). Location in B. B. High-resolution seismic reflection data showing the deformation below the contourite drift, associated to faults and fluid escapes. The normal faults here are interpreted as due to fold extrados extension from blind thrusts. Inset: in red location of MAR04 and TOPAS profiles, black rectangle corresponds to bathymetric zoom C. C. Seabed expression of pockmarks and landslide scar. Bathymetric data with contours every 50m. XB, Xauen Bank; TB, Tofino Bank; RM, Ramon Margalef Seamount.

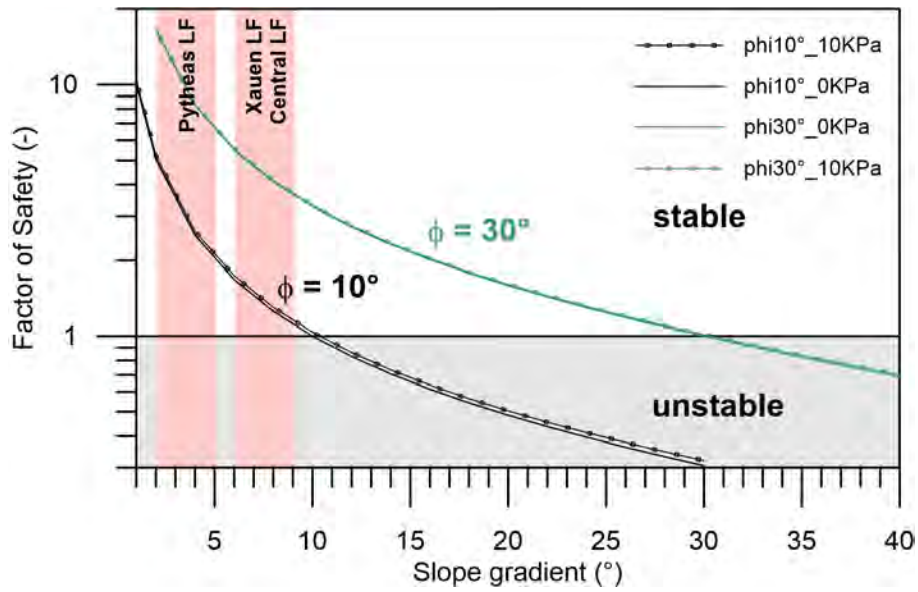


Figure 11 : Factor of safety calculations based on the infinite slope approach (FOSIS) illustrating that according to the Mohr-Coulomb criteria, the minimum slope angle required to trigger a failure is the friction angle. Calculations for three values of cohesions illustrates the restricted effects on the stability. Area of the three landslide fields (LF) according to their slope gradients are represented in pink. ϕ friction angle (ϕ); Cohesion (XKPa).

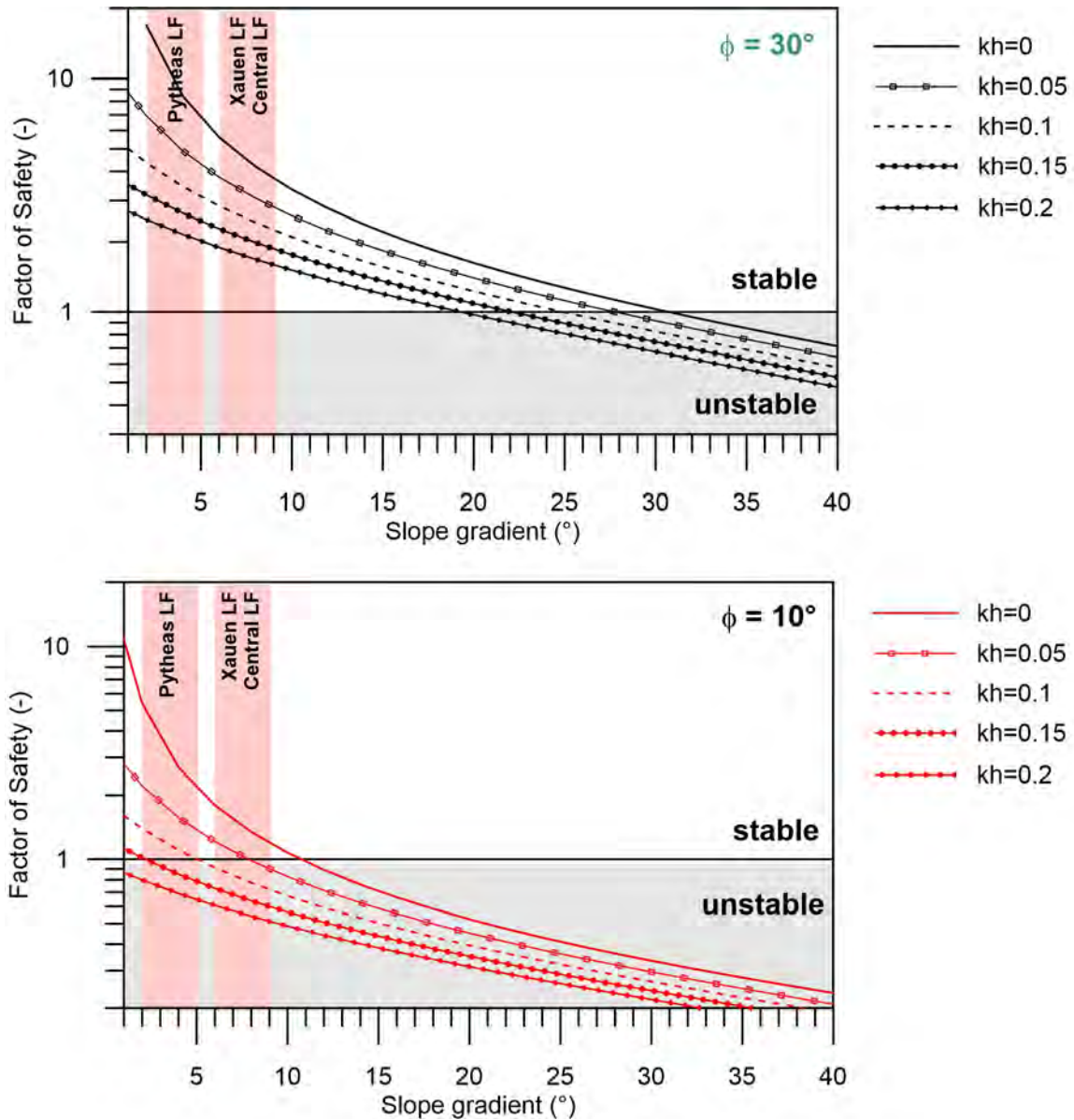


Figure 12: Factor of safety calculations based on the pseudostatic approach (FOSPS) for seismic coefficients kh from 0 to 0.2. Top: scenario of sediments with a friction angle of 30° . Bottom: scenario of sediments with a friction angle of 10° . Instability may be attained for the Xauen and Central Landslide Fields (LF) if $kh > 0.05$, and for the Pytheas LF $kh > 0.1$. ϕ friction angle; kh pseudostatic seismic coefficient.